Laboratori Nazionali di Frascati

LNF-89/077(P)
9 Novembre 1989

M.Aglietta, G.Badino, G.Bologna, C.Castagnoli, A.Castellina, B.D'Ettorre Piazzoli, W.Fulgione, P.Galeotti, G.Mannocchi, P.Picchi, O.Saavedra, G.Trinchero, S.Vernetto:

PRIMARY COSMIC RAY SPECTRUM IN THE 10^{13} - 10^{17} eV ENERGY RANGE FROM THE ANALYSIS OF MULTIPLE MUON EVENTS IN THE NUSEX EXPERIMENT

Presented by A. Castellina at the
"Topical Seminar on Astrophysics and Particle Physics"
San Miniato (Italy), May 7-11, 1989

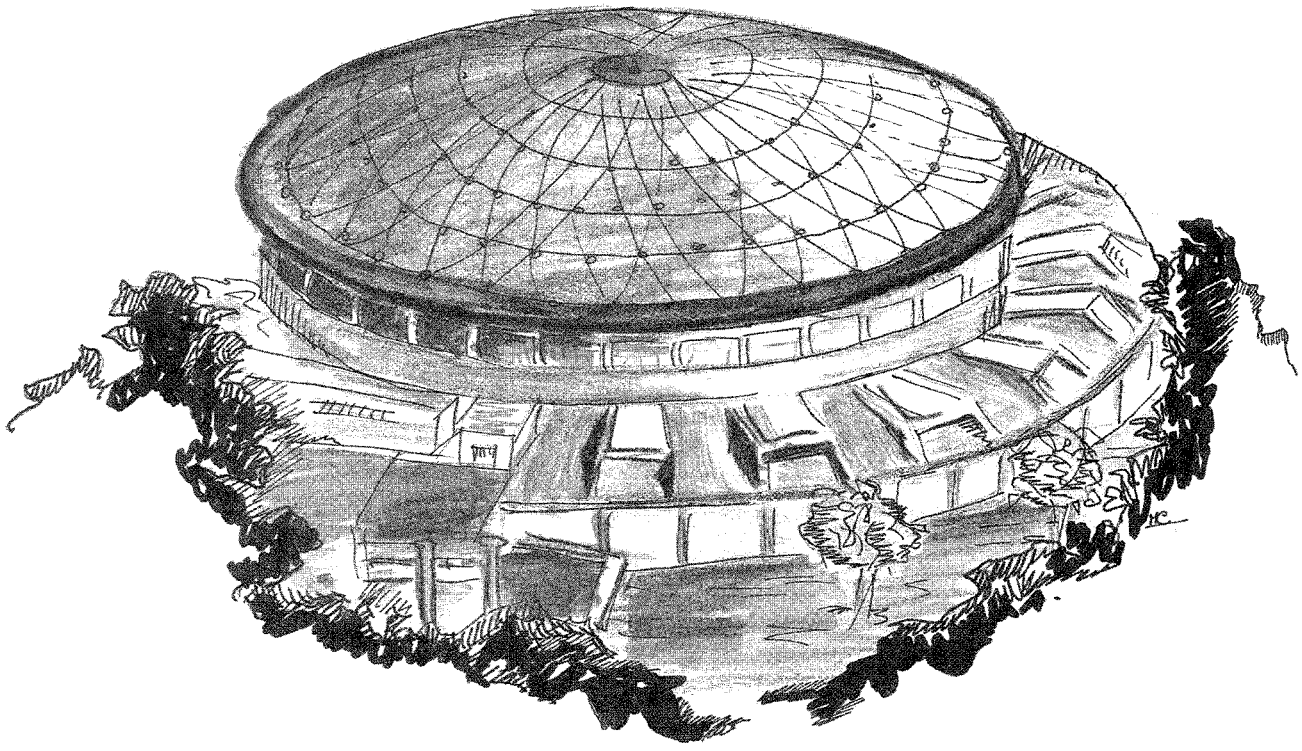

Servizio Documentazione
dei Laboratori Nazionali di Frascati
P.O. Box, 13 - 00044 Frascati (Italy)

INFN - Laboratori Nazionali di Frascati
Servizio Documentazione

LNF-89/077(P)
9 Novembre 1989

PRIMARY COSMIC RAY SPECTRUM IN THE 10^{13} - 10^{17} eV ENERGY RANGE FROM THE ANALYSIS OF MULTIPLE MUON EVENTS IN THE NUSEX EXPERIMENT

M.Aglietta[1] , G.Badino[2], G.Bologna[2], C.Castagnoli[2], A.Castellina[1], B.D'Ettorre Piazzoli[1], W.Fulgione[1], P.Galeotti[2], G.Mannocchi[1], P.Picchi[2], O.Saavedra[2], G.Trinchero[1], S.Vernetto[1]

(1) Istituto di Cosmogeofisica del CNR., Torino
(2)Istituto di Fisica Generaledell'Università di Torino

Absolute multiple muon rates have been measured in the NUSEX detector at Mont Blanc during more than 6 years of data taking. We present here a comparison with the expected rates according to different current models of primary cosmic ray composition in the energy range 10^{13}-10^{17} eV. The predictions are based on a Monte Carlo simulation of the atmospheric cascade including the most recent accelerator results on the hadronic interactions.

1.- INTRODUCTION

The primary cosmic ray beam consists of nuclei of various elemental species. The energy spectrum of each component is relevant for understanding acceleration mechanisms and the nature of cosmic ray sources. However, inspite of a continuous experimental effort, the information at energies greater than 10^{12} eV is still contraddictory. Apart from balloon data concerning the proton spectrum, information on the primary spectrum at energies greater than 10^{14} eV is obtained in an indirect way from the analysis of the properties of secondary particles produced in the atmospheric cascade. This approach has two major consequences: i) the interpretation of the results needs an accurate description of the nucleus-air nucleus interaction up to energies beyond the accelerator range; ii) the energy and type of primaries are not known

on an event by event basis and only trial compositions can be checked by comparing the experimental results to the expected ones.

A good approach to this problem is the study of the frequency distribution of high energy (> 1 TeV) muon bundles. In fact, high energy muons produced in the first steps of the atmospheric cascade can travel many kilometers and reach the ground level. The rock above the underground detector acts as an energy analyzer absorbing all the low energy air shower particles. Thus, the detection of muon bundles at very deep sites provides a picture of the first stages of the cascade. Rates of underground muons are expected to be sensitive to the energy spectrum and to the composition of the primary cosmic ray beam. The sensitivity to the composition arises from the different muon yields from nuclei of different mass and the same total energy. In fact, high energy heavy nuclei are more efficient than protons in producing TeV muons. The asymptotic behaviour of the muon yield is given by

$$N(E_o, A; > E_\mu) = A \cdot f\left(\frac{E_\mu A}{E_o}\right) \rightarrow A^{1/4} f \left(\frac{E_\mu}{E_o}\right)$$

where E_μ is the energy of a muon produced by a primary of energy E_o and mass A.

Due to the large depth of the experimental site, such that $E_\mu > 3.5$ TeV, NUSEX data allow one to study the elemental primary composition in the energy range 10^{13} - 10^{17} eV. The systematic analysis of data collected from June 1982 to December 1984 has already been described in a previous paper[1]. A suitable parametrization of the muon production based on Monte Carlo calculations has been used to relate the fluxes of multiple muons to the primary spectrum. The present analysis concerns data recorded up to December 1988 and it uses recent parametrizations obtained by means of an improved Monte Carlo simulation of the atmospheric cascade, which takes into account the most recent results from $p\bar{p}$ collider.

2. - APPARATUS

The NUSEX detector, operating since June 1982 in the garage 17 of the Mont Blanc tunnel, at a vertical depth of 5000 hg/cm^2 of standard rock, has been described in detail elsewhere[2]. Briefly, it consists of a cube 3.5 m^3 size made by 134 horizontal iron plates 1 cm thick, interleaved with planes of limited streamer tubes 1 cm^2 section. The bidimensional readout makes it possible to record the detailed spatial pattern of tracks, with a spatial resolution of 1 cm and an angular resolution of about 1 mrad for Θ and 2 mrad for Φ. The depth associated to each direction (Θ,Φ) is calculated by means of a detailed map of Mont Blanc, known to an accuracy better than 1% on average, up to zenith angle 75^o. The homogeneity of the rock both in density and in chemical composition allows a straightforward conversion to the standard rock using the result of Wright[3].

The muon rate and the response of a few test tubes to a β source are daily checked, in such a way providing a continuous monitoring of the detector and electronics efficiency and of

the stability of the gas mixture (Ar/CO_2/n-pentane, 20/40/40) used in operating the streamer tubes.

3. - EVENT SELECTION

47903 muon events were recorded in the zenith angle range (0-75°) during an effective working time of 1.5867119 10^8 sec from June 1982 to December 1988. The number of events recorded at different multiplicities is summarized in Table I. These events satisfy the following selection criteria: i)10 or more contiguous planes crossed, corresponding to a track lenght of at least 27 cm; ii) a relative angle $\Delta\Theta$ between tracks not exceeding 2.5°. Non parallel tracks with $\Delta\Theta > 2.5°$ are discarded if they approach some other tracks by less than 20 cm within a few meters above the apparatus. These simple criteria are enough to remove some locally produced particles; in this way we get a rate of 1.1 muon/hour.

From single muon events the muon intensity as a function of depth, shown in Fig. 1, is derived in the interval 4700-10700 hg/cm^2 of standard rock following the analysis of data recorded in the spark chamber experiment at Mont Blanc, garage 27 in the seventies[4]. The angular enhancement has been accounted for using the appropriate functions[5]. This curve is in excellent agreement with the one presented at the La Jolla conference[6], which was obtained using data up to December 1984 only. The single muon intensity is well represented by the relation (h in hg/cm^2 of standard rock) :

$$I(h)=(6.43 \pm 0.30)\ 10^{-7} \exp\left(\frac{-h}{814.1+0.4}\right)\ cm^{-2}\ s^{-1}sr^{-1}$$

Moreover, up to about 7000 hg/cm^2 s.r., it overlaps to the intensity points measured in the depth range 3900-7000 hg/cm^2 s.r. by the spark chamber apparatus. This gives the best evidence of the high efficiency and stability of the NUSEX detector in more than 6.5 years of operation. Physics implications from the depth-intensity curve will be discussed elsewhere.

4. - RATE CALCULATION

The rate of events in which the apparatus detects exactly n of N_μ incident muons is given by [1]:

$$\Phi_n = \Sigma_i \int J_i(A)\ P_n(E_o, A)\ dE_o$$

where $J_i(A) = K_i(A)\ E_o^{-\gamma_i(A)}$ describes the differential flux of each nuclear component present in the primary beam and $P_n(E_o, A)$ is the probability of detecting n muons of a shower resulting from the interaction of a primary with energy E_o and mass A. This probability depends on the high energy hadron interaction properties, being described in terms of the muon

number distribution around the mean at the detector depth and of their lateral distribution, including the experimental conditions (geometric acceptance and mountain pattern).

In order to follow the cascade development and the subsequent muon propagation in rock, we have used the results obtained by means of a three dimensional Monte Carlo program[7]. This cascade simulation uses an improved interaction model which includes the correlations among transverse momentum, energy and multiplicity observed at $p\bar{p}$ collider, as well as nuclear target effects derived from fixed target experiments. According to the collider data, this model predicts that Feynman scaling is rather strongly violated in the central region; only a mild breaking of the scaling law is expected in the fragmentation region. The extrapolation to the highest energies is done in the context of the inelastic "ln s" physics. A fragmentation model describes the nucleus-air nucleus interaction.

The simulation confirms that the mean number of muons N_μ is again well described, with some slight modifications, by Elbert's formula[9], but the muon number distribution around this value, $P(N_\mu)$, is no longer of Poisson type, but is better described by a negative binomial distribution. This distribution has a somewhat larger tail at large N_μ, thus the probability of high multiplicity events is increased. On the other hand, this effect is reduced in a finite size detector like NUSEX, being the events with multiplicity higher than the average one associated with broader lateral distributions. This follows from having included in the simulation the correlation between transverse momentum and event multiplicity as a function of $\sqrt{s}$ reported by CERN S $p\bar{p}$ S measurements[10]. This is crucial in determining the separation of muons, hence what fraction of muons in a shower falls within the boundary of a finite underground detector. In this context, it is worthwhile to point out that the transverse momentum distribution of charged particles derived from the model is in excellent agreement with the first data at $\sqrt{s}$ = 1.8 TeV taken at the Fermilab Tevatron collider[11].

The calculation of P_n (E_o,A) follows the prescriptions given in[1], but with the modified muon multiplicity and lateral distributions [7,8].The new P_n (E_o,A) are very close to the old ones, their values being generally larger but not exceding 30% at the highest multiplicities.

In order to get the expected multiple muon event rates, these probabilities have been folded to the primary cosmic ray spectrum described as a superposition of five mass groups of nuclei (p,He, CNO group, Mg-Si group, Fe group). Reasonable primary compositions have been considered in order to investigate the sensitivity of multiplicity distributions to the fraction of each nuclear species present in the primary beam.

5. - PRIMARY SPECTRA AND COMPOSITION

Different models for the primary cosmic rays have been proposed in order to explain the results of air shower or emulsion experiments.

Generally speaking, these models divide into two categories according to the evolution of the mixture of primary elements over the knee region, between 10^{15} and 10^{16} eV. If the origin

of the knee is interpreted as the leakage of cosmic rays from the Galaxy, the primary cosmic rays would change their composition to become heavy-nuclei enriched across the bend region. Support to these models comes from various phenomena interpreted as due to high-mass primaries, such as fast development of EAS, low frequency of γ ray families and delayed hadrons near air shower core. Typical models illustrating this point of view are those proposed by the Maryland group ('Maryland composition')[12] and the primary cosmic ray composition inferred from the intensities of γ families observed both at Mt.Kanbala and Mt.Fuji ('p-poor composition')[13].

On the contrary, there are other experimental evidences that protons give a significant contribution at energies around and over the knee. From the analysis of hadron intensities at mountain altitudes, Kempa and Wdowczyk[14] deduced that the average mass of the primaries does not increase significantly in the knee region and obtain a primary cosmic ray spectrum by an extrapolation of the directly measured spectra of the elemental species with a single constant differential slope ('constant mass composition').

The two-populations model proposed by Linsley invokes a new proton source taking over at high energy and cancelling the effect of the conventional proton bend ('Linsley composition')[15]. In this way it is possible to account for the flattening of the all particle intensity in the region 10^{14}-10^{16} eV before the steepening found at higher energies.

These models assume for each primary elemental species a power spectrum $E^{-\gamma}$ with constant slope up to a fixed magnetic rigidity R_c (GeV/nucleon), beyond which the spectra steepen due to an increased rate of leakage out of the Galaxy. The break for nuclei different from protons is set at total energy R_c (GeV/nucleus). Beyond this energy, all components assume the same slope in order to agree with air shower data. The basic parameters are summarized in Table II.

One may notice that a substantial arbitrarity exists in modelling the spectra around and over the bending point, being the accuracy of air shower measurements rather poor and the procedure in determining the primary energy from the measured size not free from uncertainties. This explains why the proposed models differ not only in the relative fraction of the elements but also in the shape of the all-particle spectrum beyond 10^{15} eV, as shown in Fig. 2, where the expectations from the p-poor and the Linsley compositions are compared. The fraction of each component and the all-particle flux at energies from 10^{13} to 10^{17} eV are summarized in Table III.

6. - COMPARISON WITH OBSERVATIONS

The experimental data on the absolute rates of multiple muons are compared in Fig.3 with the simulation results obtained when different composition models are used. The measured integral rates N(> m) are compared in Table IV with the predictions of the examined models.

We observe a general and remarkable agreement between data and calculations, mainly for low multiplicity events. It is important to underline that this comparison is done without any normalization procedure; on the other hand, an inspection of the curves in Fig. 3 and of the numerical values in Table IV shows that none of the trial compositions is able to reproduce the whole set of experimental data.

Finally, it should be noted that compositions with an increased fraction of high mass primaries do not necessarily predict an enhanced rate of high multiplicity muon bundles (for instance, compare the p-poor and constant mass composition). In the following, a detailed analysis is devoted to elucidate these aspects.

Events of low (m = 1,2) and high (m ≥4) multiplicities are originated by primaries of different mass and energy. Single and double muon events are mainly produced by protons and helium nuclei in the energy region around 10^{14} eV, as shown in Fig. 4, where the contribution of each primary component to the rate of multiple muons at different multiplicities is plotted as a function of the total energy E_0. The curves refer to the p-poor (Fig. 4a) and Linsley (Fig. 4b) models.

The slight discrepancy in the rate of single and double muons can be attributed to a non correct normalization of the proton and helium nuclei fluxes in this energy region. About 90% of the single muon events are originated by interactions of protons (~ 75%) or helium (~ 15%) nuclei as shown in Fig. 5, where the expected contributions according to the p-poor and the constant mass composition spectra are displayed. This result holds irrespectively of the considered model, apart from the Linsley composition, where the proton contribution is dominant for all multiplicities, Fig. 4 : 87% to the single muons rate, 71% to the double muon one and from 65% to 60% for higher multiplicities. According to these figures, the rate of single muon events appears to be almost insensitive to the details of the primary composition and depends mainly on the proton flux in the low energy range, 5 10^{13}-2 10^{14} eV.

In this energy region both physics and astrophysics are known accurately enough; the observed agreement between measured and calculated single muon rates shows that the details of topography and rock density, as well as detector geometry, have been folded with good accuracy into the calculation of the probability $P_n(E_0, A)$. This precision was not reached in the analysis of previous experiments, where only the ratios of multiple to single muon rates were taken into account[16].

The constant mass composition very well explains the experimental rates of single and double muon events. For comparison, the primary proton intensity expected from the Maryland composition is 35% lower at 10^{14} eV, reflecting in an expected single muon rate 27% lower than the experimental one.

The p-poor composition is in slight disagreement with both single and double muon rates, the discrepancy being essentially originated by the rather low rigidity cutoff, such that the proton and helium spectra start to bend at energies just around 10^{14} eV. On the opposite side,

the large proton flux predicted by Linsley reflects in a yield of single and double muons about 15-20% higher than the observed rate.

Events of increased multiplicity sample primaries of higher energies, up to 10^{17} eV. The effect is enhanced because the finite size of the detector sharply reduces the observed muon multiplicities and correspondingly increases the average energy required for the generation of a muon group. While the production of triples is equally shared among the various primary nuclei, the main contribution to the rate of m ≥4 muon groups comes from the heaviest nuclei, the Mg and Fe groups, at energies well beyond 10^{15} eV, as shown in Figs. 4 and 5. The only exception is represented, as already mentioned, by the Linsley composition.

The lack of statistics prevents one to individually compare the rates of each multiplicity, but the integral rate N(≥m) constitutes an excellent signature for the absolute heavy nuclei content in the primary beam.

The differences among the predictions of the various models are due not only to the chosen slopes of different primary groups, but also to the predicted all particle flux. For example, the relative fraction of heavy nuclei (Mg and Fe) in the p-poor composition is about 62% beyond 10^{16} eV, while according to the constant mass composition it increases from 36% at 10^{16} eV up to 49% at 10^{17} eV. However, in the latter model, the assumed all particle spectrum is remarkably higher. The overall effect is that the integral rate N(≥ 4) in the constant mass composition model is higher than the prediction of the p-poor composition. The experimental rate is lower than expected by both predictions, even if it differs by only about two standard deviations from the expectation of the p-poor model (see Table IV).

Likewise, the enhanced flux of heavy nuclei expected in the Maryland composition (Table III) explains why this model is unable to reproduce the experimental data for m > 3. On the other hand, the 22% deficit in the expected single muon rate compared to the experimental one indicates that this composition is unbalanced, being too poor of light nuclei below 10^{15} eV and too rich of heavy primaries beyond the knee.

The Linsley composition is poor of heavy nuclei, nevertheless the yield of muon bundles of high multiplicity (m ≥ 4) is abundant and comparable to the expectations of high mass enriched compositions. As already mentioned, protons provide the dominant contribution to all multiplicities (Fig.4). In fact in this model an enhanced flux of protons in the energy range 5 10^{15}-10^{17} eV compensates their low efficiency in producing high multiplicity events. As a consequence the all particle flux in this energy region is a factor of two higher than the one expected according to the p-poor composition (Fig. 2).

7. - CONCLUSIONS

NUSEX detector has been working with high efficiency and stability for many years, providing a clean and statistically significant amount of multiple muon events produced by primaries of energy up to 10^{17} eV. The experimental data are in substantial agreement with the

simulation results, which reproduce them at a level better than 20% in the energy region around 10^{14} eV, where the primary beam and the hadronic interactions are rather well known. This is a good evidence that the whole procedure of data reduction and simulation does work.

However, the analysis done in the previous sections shows that different models of primary composition can provide multiple muon rates yet consistent with data, so that the details of primary spectra cannot be resolved.

In NUSEX experiment, low multiplicity events are sensitive to the absolute flux of protons and helium nuclei around 10^{14} eV, while the rate of high multiplicity events depends essentially on the absolute content of heavy primaries. These fluxes can be accomodated in various different ways according to the choice of the bending point, spectral index γ and total flux. Thus, an unambiguous measurement of the total flux beyond 10^{15} eV or, better, a contemporary measurement of the primary energy (for instance, sampling the electron component of the air shower) on an event by event basis could provide further constraints to discriminate among different models[8].

It should be stressed that the low sensitivity to different compositions does not depend on the small size of the apparatus. A simulation brought on using a bigger apparatus (about 120 m^2) shows that the difference between two opposite compositions, like the p-poor and the constant mass model ones, is not bigger than 1 standard deviation, after one year of data taking, even at high multiplicities.

If the p-poor model is taken as a reference, NUSEX data suggests a reduction of the heavy primaries flux respect to the assumed one. A decrease of about 30% of the Mg-Si and Fe fluxes at energies beyond 5 10^{15} eV could restore a fair agreement with the experimental data at high multiplicities.

This may be achieved by both decreasing the spectral index and moving the normalization. When applied, these operations tend to reduce the rate of low multiplicities; this effect can be compensated increasing the rigidity cutoff, together with a slight renormalization of the flux of proton and helium nuclei. The result of such an adjustment is given in Table V, where the spectral index of the Mg-Si group has been increased according to recent suggestions[17]. The normalization of the Mg-Si and Fe groups has been chosen following the prescriptions given at ICOBAN '84 [18]. The rigidity cut-off R_c is set to 5 10^5 GeV/nucleon. The all particle flux remains substantially unchanged.

This model provides a set of multiple muon rates in excellent agreement with the measured one. Differences in Φ_i (i=1,2,3) and $N(\geq 4)$ do not exceed 10%, comparable to the estimated uncertainties in the shower simulation. One should note again that some arbitrarity exists in modelling the spectra. However, NUSEX composition suggest that proton spectrum would start to bend at energies larger than 10^{14} eV and that the fraction of heavy nuclei (Mg-Si plus Fe groups) to the total is about 27% and 40% at energies 10^{15} and 10^{16} eV respectively (the all-particle flux at these energies is 2.60 10^{-12} and 3.74 10^{-15} $m^{-2}s^{-1}sr^{-1}$ GeV^{-1}).

REFERENCES

1. G.Bologna et al., Il Nuovo Cimento 8C (1985) 76.
2. G.Battistoni et al., Nucl.Instr. and Methods. A245 (1986) 277.
3. A.G.Wright, Proc.of the 13th ICRC, Denver,vol.3 (1973) 1709.
4. L.Bergamasco et al., Il Nuovo Cimento 6C (1983) 569.
5. A.Castellina et al., Il Nuovo Cimento 8C (1985) 93.
6. G.Battistoni et al., Proc.of the 19th ICRC, La Jolla, vol.2 (1985) 158.
7. H.Bilokon, B.D'Ettorre Piazzoli, C.Forti, T.Gaisser, L.Satta, T.Stanev, in print.
8. B.D'Ettorre Piazzoli , Surface and underground experiments at the Gran Sasso, Proc.of the Les Rencontres de Physique de la Vallée d'Aoste (1988), 239.
9. T.Gaisser and T.Stanev, Nucl.Instr.and Meth. A235 (1985) 183.
10. F.Ceradini et al.,UA1 Coll.,Proc. Int. Europhysics Conf. on High Energy Physics, Bari (1985) 363.
11. F.Abe et al., Phys.Rev.Lett. 61 (1988) 1819.
12. G.B.Yodh et al., Phys.Rev. D29 (1984) 892.
13. R.Ren et al., Phys.Rev. D38 (1988) 1404.
14. J.Kempa and J.Wdowczyk, Jour.Phys.G: Nucl.Phys., 9 (1983) 1871.
15. J.Linsley, Proc. of the 18th ICRC, Bangalore 12 (1983) 135.
16. W.Elbert, T.Gaisser and T.Stanev, Phys.Rev.D27 (1983) 1448.
17. J.M.Grunsfeld et al., Astr.Journ. 327, (1988) L31.
18. G.B.Yodh,T.K.Gaisser and T.Stanev, The Physics of Multimuons, in: ICOBAN '84, Park City, Utah (1984).

TABLE I - Number of recorded events at each different multiplicity m.

m	EVENTS
1	47219
2	601
3	60
4	11
5	8
6	3
7	1

TABLE II - Normalization factor K ($m^{-2}s^{-1}sr^{-1}(GeV/nucleus)^{-1}$), slope, cutoff energy E_c (GeV) and slope after the cutoff for the four used models.

GROUP	K	γ	E_c	γ ($E>E_c$)
P-poor composition				
p	$1.51\ 10^4$	2.70	$1.0\ 10^5$	3.0
α	$7.02\ 10^3$	2.70	$2.0\ 10^5$	3.0
CNO	$2.68\ 10^3$	2.61	$7.0\ 10^5$	3.0
Mg	$2.93\ 10^3$	2.62	$1.4\ 10^6$	3.0
Fe	$8.56\ 10^2$	2.50	$2.8\ 10^6$	3.0
Maryland composition				
p	$1.98\ 10^4$	2.75	$3.0\ 10^5$	3.35
α	$1.03\ 10^4$	2.77	$6.0\ 10^5$	3.37
CNO	$2.15\ 10^3$	2.60	$2.1\ 10^6$	3.20
Mg	$1.14\ 10^3$	2.50	$4.2\ 10^6$	3.10
Fe	$5.95\ 10^2$	2.50	$8.4\ 10^6$	3.10
Constant mass composition				
p	$1.72\ 10^4$	2.71	$2.0\ 10^6$	3.00
α	$9.20\ 10^3$	2.71	$4.0\ 10^6$	3.00
CNO	$6.20\ 10^3$	2.71	$1.4\ 10^7$	3.00
Mg	$9.20\ 10^3$	2.71	$2.6\ 10^7$	3.00
Fe	$6.20\ 10^3$	2.71	$5.2\ 10^7$	3.00
Linsley composition				
p	$2.60\ 10^4$	2.73	$1.0\ 10^5$	
	$1.84\ 10^3$	2.50	$1.0\ 10^7$	3.02
α	$8.16\ 10^3$	2.73	$1.0\ 10^6$	3.23
CNO	$5.65\ 10^3$	2.73	$3.5\ 10^6$	3.23
Mg	$7.30\ 10^3$	2.73	$7.0\ 10^6$	3.23
Fe	$6.33\ 10^3$	2.73	$1.3\ 10^7$	3.23

TABLE III - All-particle flux ($m^{-2}s^{-1}sr^{-1}GeV^{-1}$) and percentage contribution of each primary component for the four considered models, at five different primary energies E_0.

E_0(eV)	10^{13}	10^{14}	10^{15}	10^{16}	10^{17}
p-poor composition					
total flux	$6.30\ 10^{-7}$	$1.44\ 10^{-9}$	$2.67\ 10^{-12}$	$3.33\ 10^{-15}$	$3.33\ 10^{-18}$
p	33.1	33.1	17.8	14.3	14.3
He	15.4	15.4	10.2	8.2	8.2
CNO	16.6	16.6	19.1	15.3	15.3
Mg	16.1	16.1	20.9	19.1	19.1
Fe	18.8	18.8	32.0	43.1	43.1
Maryland composition					
total flux	$5.43\ 10^{-7}$	$1.26\ 10^{-9}$	$2.76\ 10^{-12}$	$4.58\ 10^{-15}$	$3.47\ 10^{-18}$
p	27.9	27.9	11.0	3.0	3.0
He	11.5	11.5	6.6	1.7	1.7
CNO	17.0	17.0	19.6	11.7	11.7
Mg	28.6	28.6	41.3	46.7	46.7
Fe	14.9	14.9	21.5	37.0	37.0
Constant mass composition					
total flux	$6.94\ 10^{-7}$	$1.35\ 10^{-9}$	$2.64\ 10^{-12}$	$4.53\ 10^{-15}$	$5.90\ 10^{-18}$
p	35.8	35.8	35.8	29.6	22.7
He	19.2	19.2	19.2	19.4	14.9
CNO	12.9	12.9	12.9	14.6	14.6
Mg	19.2	19.2	19.2	21.7	26.1
Fe	12.9	12.9	12.9	14.6	21.7
Linsley composition					
total flux	$6.42\ 10^{-7}$	$1.20\ 10^{-9}$	$2.98\ 10^{-12}$	$7.24\ 10^{-15}$	$6.43\ 10^{-18}$
p	48.6	48.6	61.6	80.3	86.3
He	15.3	15.3	11.4	2.8	1.8
CNO	10.6	10.6	7.9	3.6	2.4
Mg	13.7	13.7	10.2	6.6	4.4
Fe	11.8	11.8	8.9	6.8	5.1

TABLE IV - Experimental integral muon bundles rate (column 6) in comparison to the expected values

N(>m)	LINSLEY	C.M.C.	MARYLAND	P-POOR C.	NUSEX
1	55650.98	47632.22	37469.87	44363.15	47903 ± 219
2	750.75	665.55	658.16	569.90	684 ± 26
3	98.61	97.51	112.33	81.19	83 ± 9
4	27.52	30.54	34.10	25.02	23 ± 5
5	11.10	13.25	13.79	10.48	12 ± 3
6	5.23	6.57	6.45	5.22	4 ± 2
7	2.63	3.10	2.85	2.60	1 ± 1

TABLE V - Normalization factor K ($m^{-2}s^{-1}sr^{-1}(GeV/nucleus)^{-1}$), slope,cutoff energy E_c (GeV) and slope after the cutoff for the composition suggested by our experimental data

Group	K	γ	E_c	$\gamma (E>E_c)$.
p	$1.6\ 10^4$	2.70	$5.0\ 10^5$	3.0
α	$8.0\ 10^3$	2.70	$1.0\ 10^6$	3.0
CNO	$2.7\ 10^3$	2.61	$3.5\ 10^6$	3.0
Mg	$8.1\ 10^3$	2.73	$7.0\ 10^6$	3.0
Fe	$1.4\ 10^3$	2.60	$1.4\ 10^7$	3.0

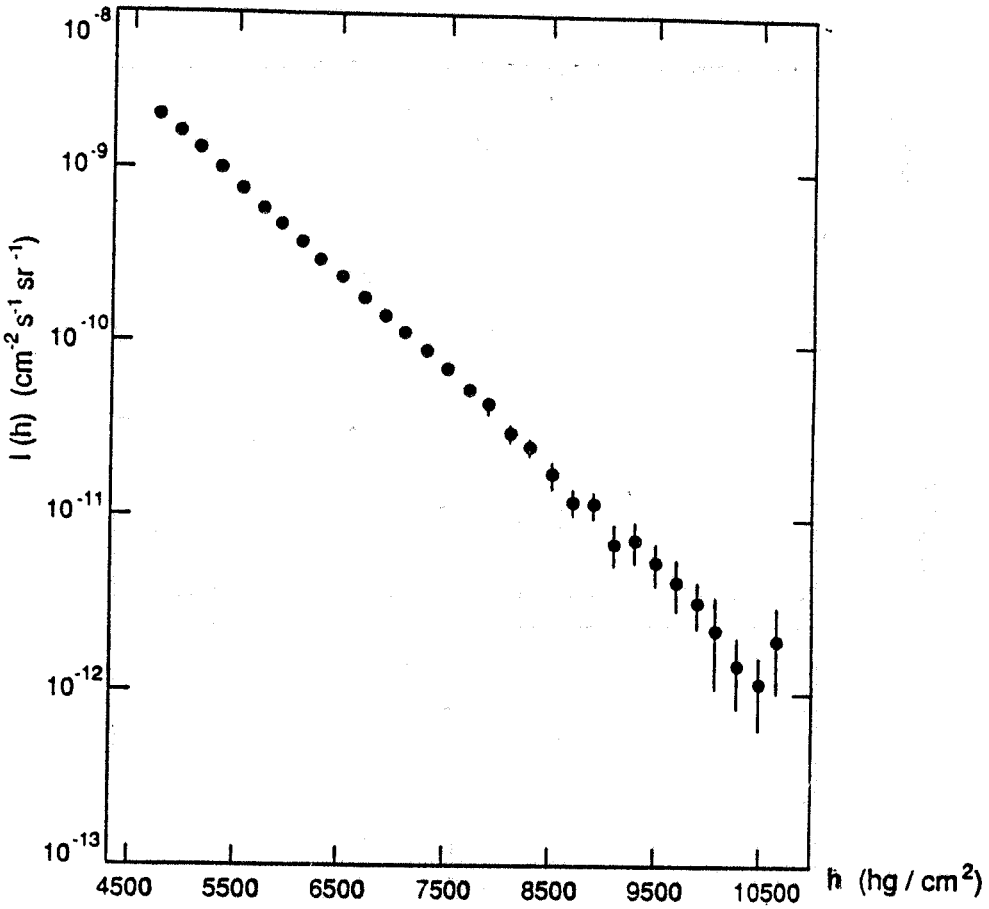

FIG. 1 - Single muon intensity as a function of depth.

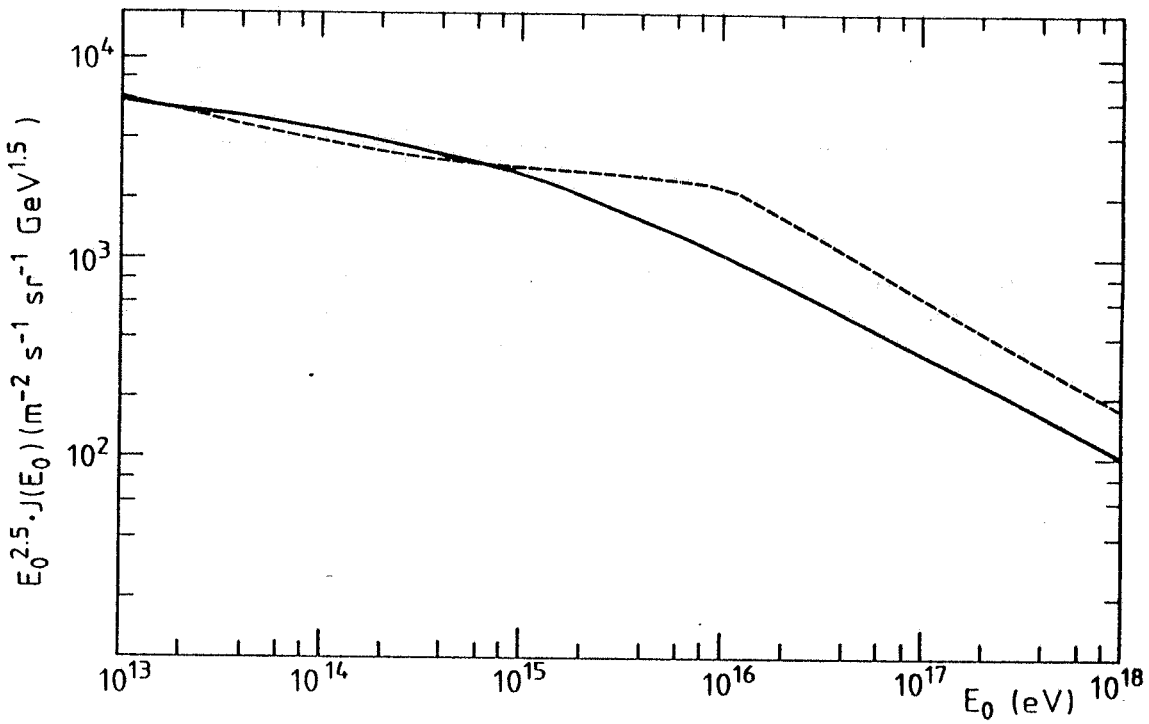

FIG. 2 - All-particle energy spectrum. Full line: p-poor composition; dashed line: Linsley composition.

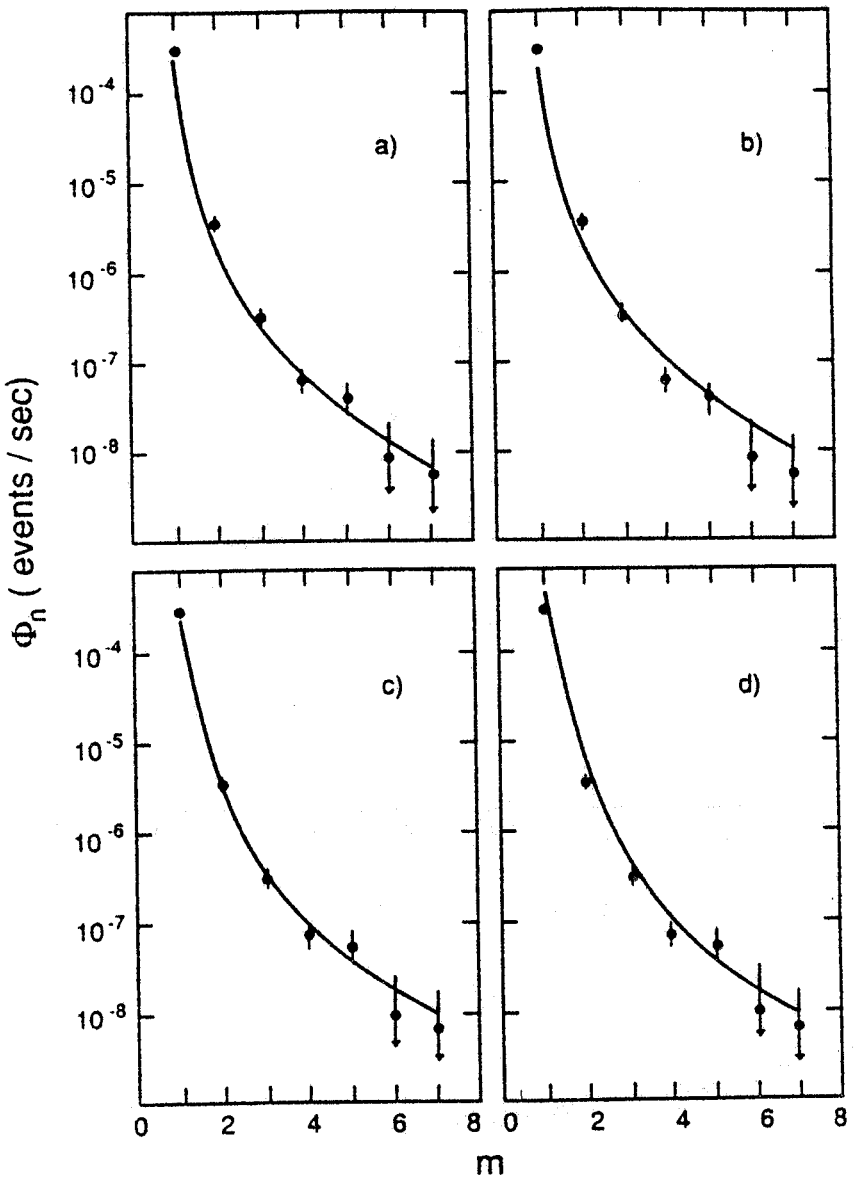

FIG. 3 - Comparison of the experimental muon bundle rate to the expected one according to the four considered models: a) p-poor model; b) Maryland model; c) constant mass model; d) Linsley model.

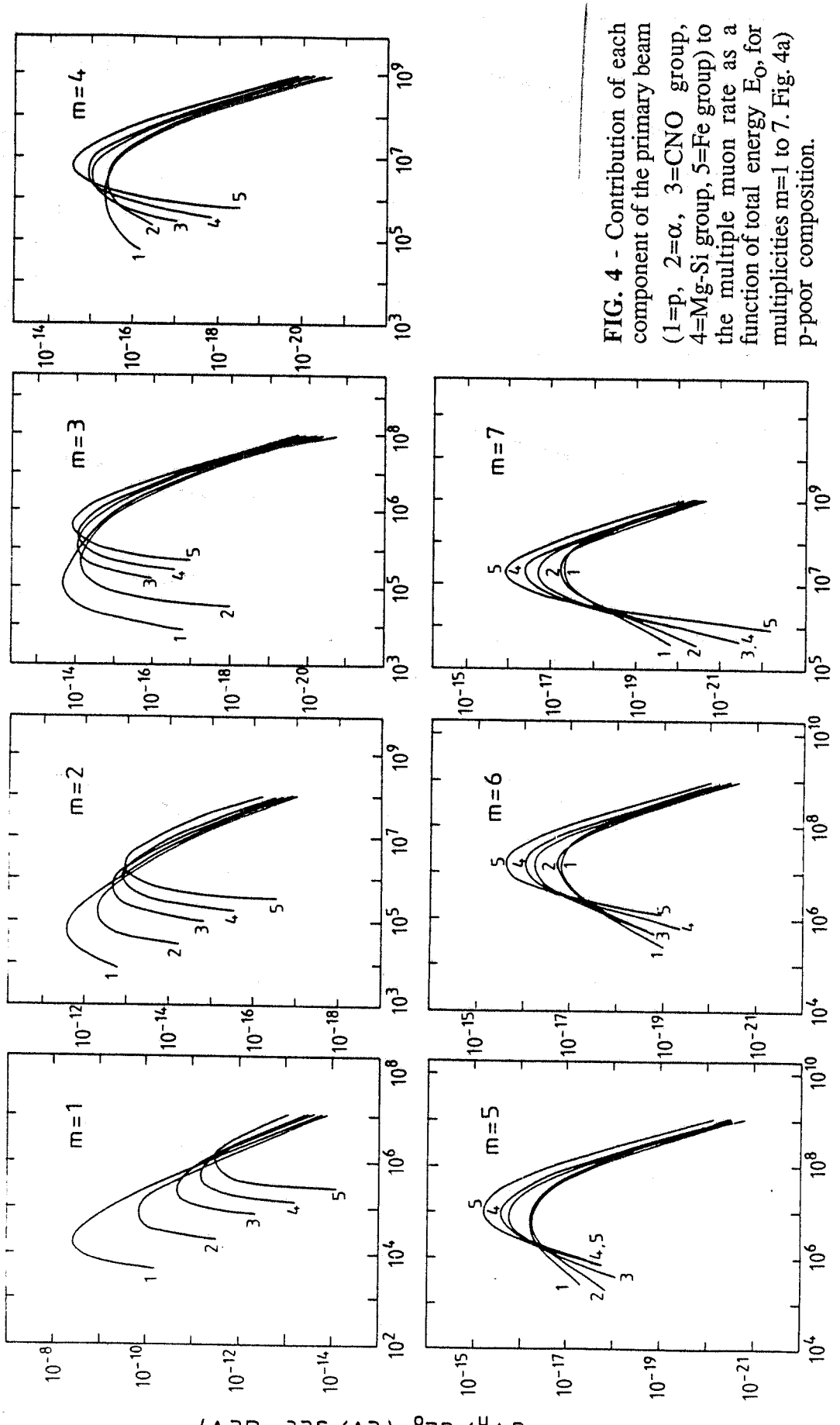

FIG. 4 - Contribution of each component of the primary beam (1=p, 2=α, 3=CNO group, 4=Mg-Si group, 5=Fe group) to the multiple muon rate as a function of total energy E_o, for multiplicities m=1 to 7. Fig. 4a) p-poor composition.

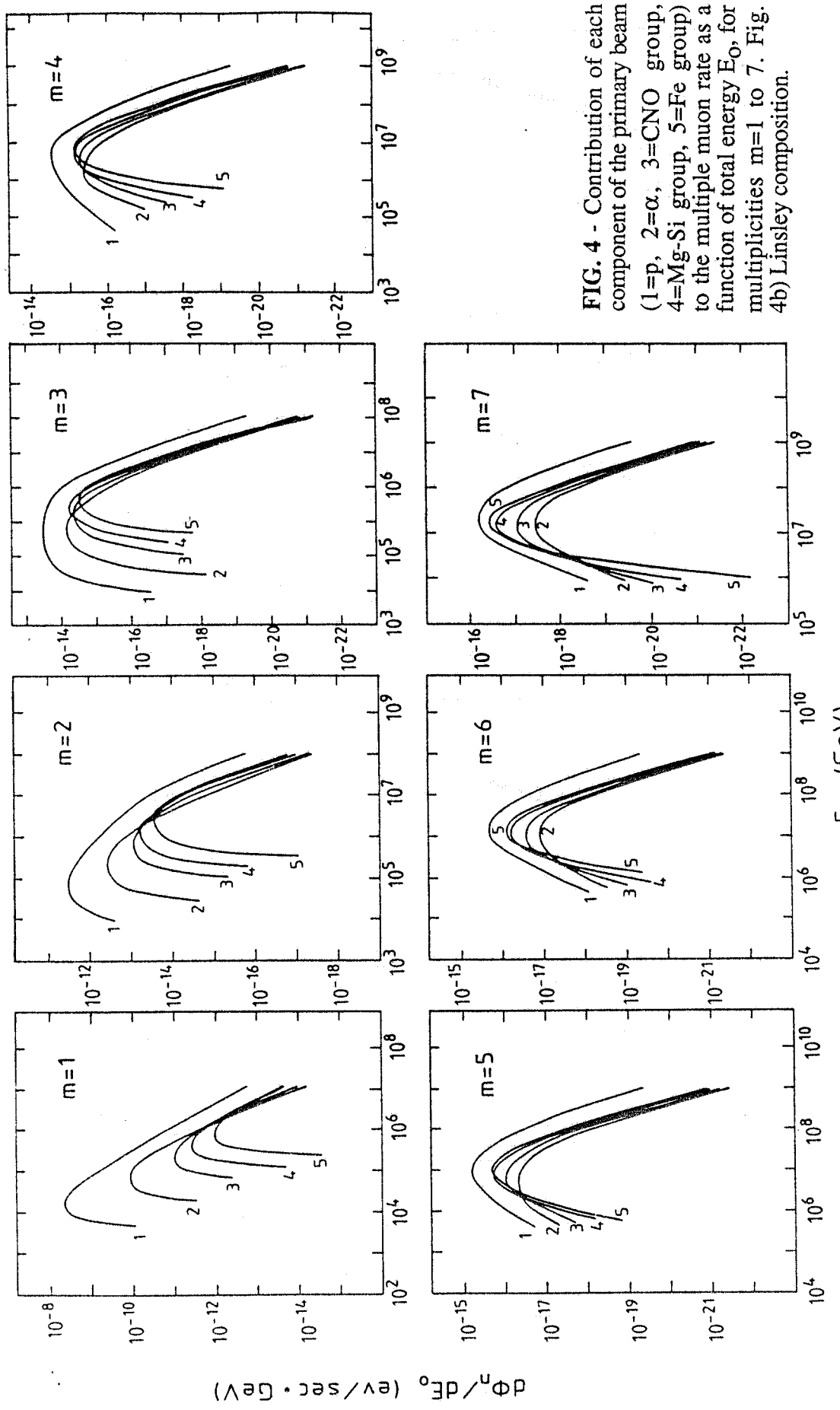

FIG. 4 - Contribution of each component of the primary beam (1=p, 2=α, 3=CNO group, 4=Mg-Si group, 5=Fe group) to the multiple muon rate as a function of total energy E_o, for multiplicities m=1 to 7. Fig. 4b) Linsley composition.

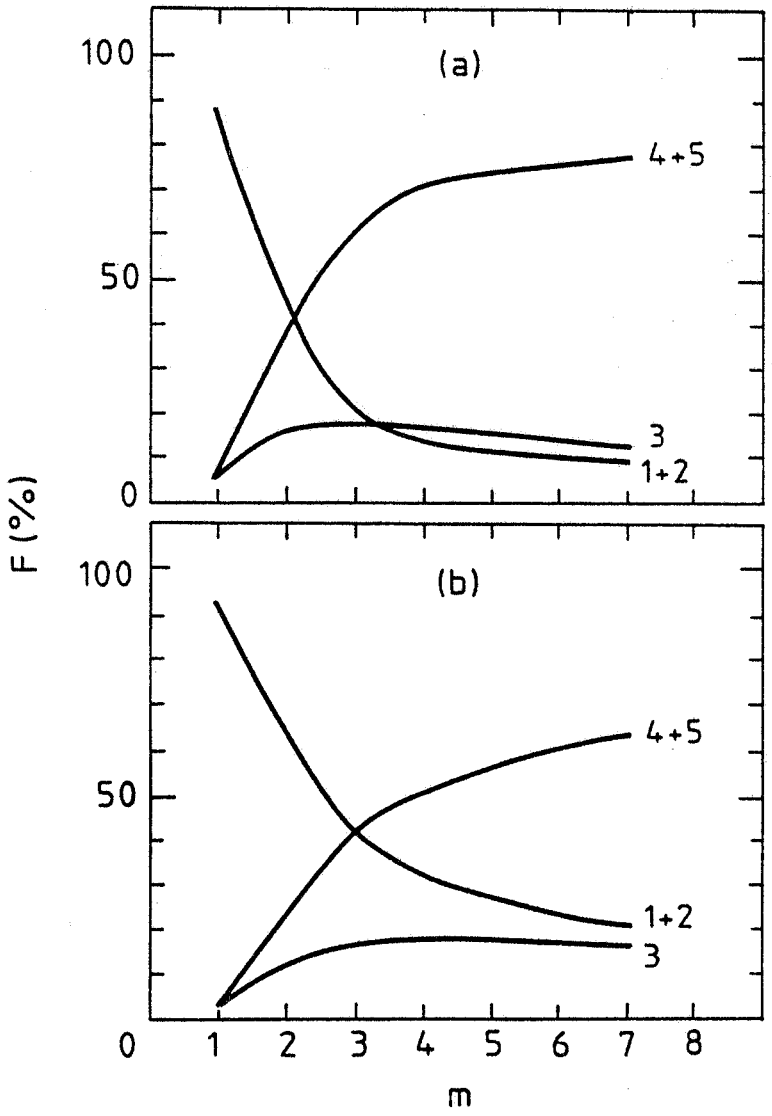

FIG. 5 - Expected contribution (%) of the different primary groups of nuclei (1+2=p+α, 3=CNO group, 4+5=Mg-Si + Fe group) to muon bundles events of multiplicity m. Fig.5a) p-poor composition; Fig.5b) constant mass composition